IOP Conf. Series: Materials Science and Engineering **232** (2017) 012068 doi:10.1088/1757-899X/232/1/012068

The process of gas-dynamic design of pneumatic braking system using the baseline compressor

Y Novikova[1], G Popov[1], E Goriachkin[1], O Baturin[2], V Zubanov[1]

[1] Junior Researcher, Samara National Research University, Samara, Russia
[2] Associate Professor, Samara National Research University, Samara, Russia

E-mail: y.d.novikova@gmail.com

Abstract. The article presents the results of work on the design of the air brake for testing of industrial gas turbine engines with free turbine. Designing of the air brake was performed on the basis of existing units using the program CFD - simulation Numeca FineTurbo. During the design the air brake arrangement was determined, which allows to utilize the required power to the shaft of the free turbine, increases stall margin of the air brake by waisting of the meridional flow channel. It was also made designing of the outlet guide vane to remove the residual twist. Unified nozzle also was designed to provide the air brake work at necessary points on the characteristic.

1. Introduction

Testing of gas-turbine engines (GTE) is an essential part of their life cycle. Tests are carried for the newly created engines, and for the serially produced engines before their delivery to the customer.

During testing the industrial GTE, designed to drive electric generators, compressors pumps and etc. there is a problem of utilization and measurement of generated power.

Air brake device is an air compressor [1]. Air brake utilizes the power generated by GTE by compressing the air. Creation and design of compressors is a difficult and expensive task [2]. This explains the high cost of GTE air brake devices. However, if existing compressor is use as the air brake, it can significantly reduce the cost of developing of the air brake, and also reduce the time of its creation. This was the way it was decided to go in design of the air brake for testing of industrial gas turbine engines in for the JSC "Kuznetsov [3].

As part of the work it was required to design the air braking system for a family of industrial GTE. The air brake intended to dispose of power on the free turbine shaft. According to the technical task the air brake had to provide power utilization of 25 MW at a rotor speed of 5000 rev / min and the power of 32 MW at the rotor speed of 5500 rev / min. To reduce the cost of development it was supposed to complete the project on the basis of the existing compressor (the base compressor) (Figure 1). Base compressor is a low-pressure compress (LPC) or of a bypass turbojet engine, developed and produced by JSC Kuznetsov. One of the key requirements in the development of the air brake was a minimal redesign of the base compressor, as well as the minimum production of new parts.

The development of the air brake was carried out on basis of the base compressor. For this reason it was decided to use CFD-modeling method, which was implemented in the software package NUMECA FineTurbo [4].

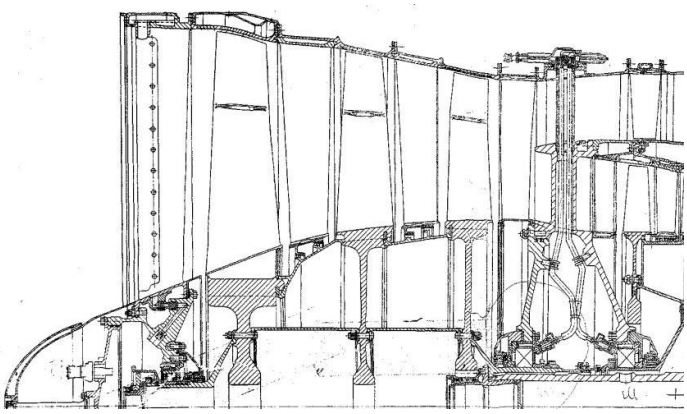

Figure 1. Geometry of the base compressor.

2. Numerical model of the base compressor and its validation

Before using CFD-programs for research, as a rule, verification of calculation models is performed [5]. For this reason, at the first step of the work the validation of numerical models was performed. Validation of numerical models is performed due to comparison between the calculated characteristics of the base compressor and experimental characteristics.

The numerical model of the base compressor was created in the software NUMECA FineTurbo [6] and it consisted of rotor blade domains (RB1, RB2, RB3), guide vanes domains (GV1, GV2, GV3, GV3a), inlet guide vanes domain (IGV), and bearing strut domains in the outer and inner duct (Figure 2). The created model took into account the radial clearance, as well as anti-vibration flange at the rotor blades.

The block-structured grid was made in the program Numeca Autogrid 5. Element size, which is closest to the walls of the computational domain (blade surfaces, struts, meridional shrouds, etc.), is provided the value of the parameter y+ equal to1. The elements number of calculated mesh of the rotor blade domains was about 840 thousand elements, mesh of the guide vanes domains - about 300 thousand elements. The total size of the grid of the entire model was 5.5 million items (Figure 3).

The turbulence model Spalart-Allmaras was used during calculation. The calculation of rotor blade domains was carried out in a rotating coordinate system. The rotational speed was 5000 rev / min. To transfer data between domains the interface Full Non Matching Mixing Plane was used, which averaged flow parameters in the circumferential direction.

At the inlet to the calculated model the parameters of air were set: the total pressure of 101325 Pa and the total temperature 288,15 K. At the outlets of the first and second ducts the massflow rates were set which correspond to the required characteristics point (Figure 2).

Using the created computational model the characteristics of the base compressor were calculated (Figure 4, 5). According to the results of the characteristics calculation, these dependencies were plotted:

1. The compressor total pressure ratio in the first duct of the base compressor vs total massflow rate $\pi_I^* = f(G_{A\Sigma g})$ (curve I contour - figure 4*);*
2. The compressor total pressure ratio in the second duct of the base compressor vs total massflow rate $\pi_{II}^* = f(G_{A\Sigma g})$ (curve II contour - figure 4*);*
3. The efficiency of the first duct vs the total massflow rate $\eta_I^* = f(G_{A\Sigma g})$ (curve I contour - figure 4*);*
4. The efficiency of the second duct vs the total massflow rate $\eta_{II}^* = f(G_{A\Sigma g})$ *(*curve II contour - figure 4*);*
5. The total capacity of the air brake vs the relative massflow rate $N = f(G_{A\Sigma g})$ *(*figure 5*).*

Plotted calculated dependencies were compared with experimental data. By comparing the results the following conclusions were made:

1. The characteristics obtained by calculation, repeat the qualitative nature of the experimental characteristics;
2. Quantitative error in determining the capacity is 10%;
3. Quantitative error in determining the flow rate is 4.6%;
4. Created computational model can be used in research on the condition of correction of the calculated characteristics on the value of the identified errors.
5. Base compressor does not provide the required power utilization at the operation mode 5000 rev / min.

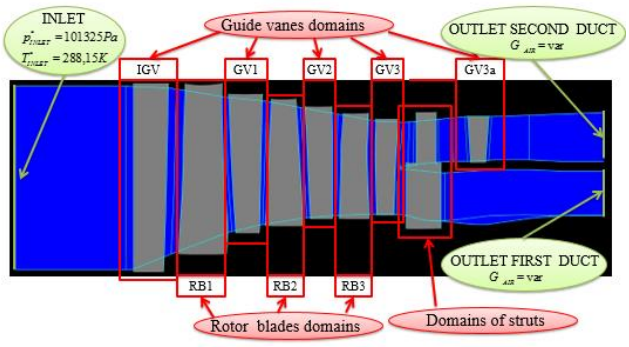

Figure 2. Computational domain of the base LPC.

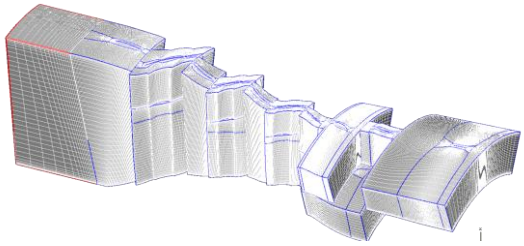

Figure 3. Finite element mesh for the computational model of the base LPC.

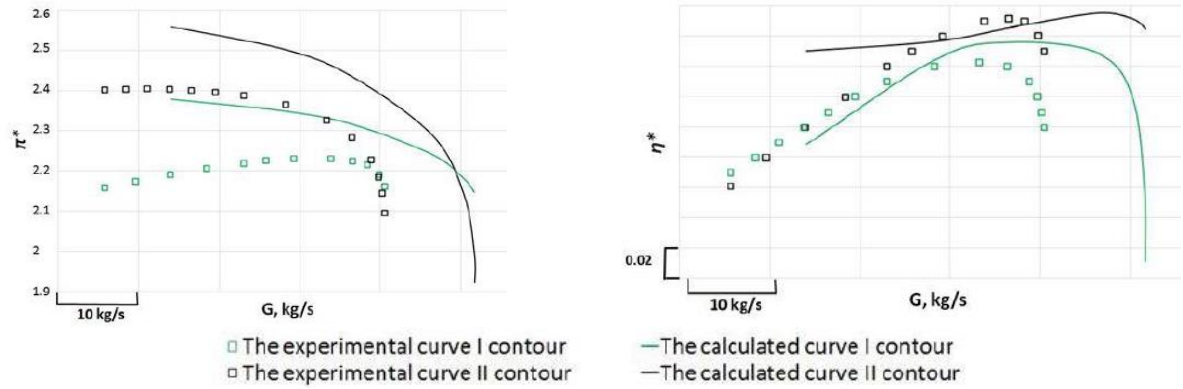

Figure 4. Head characteristics and efficiency for the base LPC.

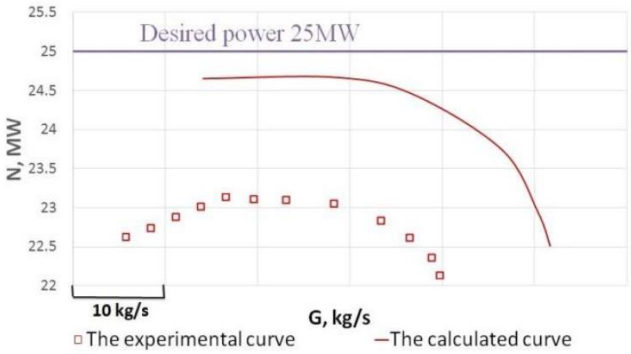

Figure 5. The dependence of the air brake total power vs the relative massflow rate for the base LPC.

3. Four - stage air

Since the base compressor is not able to provide the required power utilization at operation modes of 5000 rev / min and of 5500 rev / min (Figure 5) it was decided to make its modernization, by adding of the additional booster stages to it. For this reason, it was decided to make four stage air brake by duplication of the third stage to reduce the cost of construction (AB_RB4). However, the design of the fourth guide vanes was the same with the design of the third guide vanes. The blades of a fourth rotor blade were obtained by cropping of the third blade wheel so that the shroud of a flow channel of the fourth stage was cylindrical (AB_RB4_CD). This design allows producing the new stage from already available components with minimal modifications.

Designed variant of air brake is shown on Figure 6.

The characteristics were calculated for this variant (Figure 7, 8).

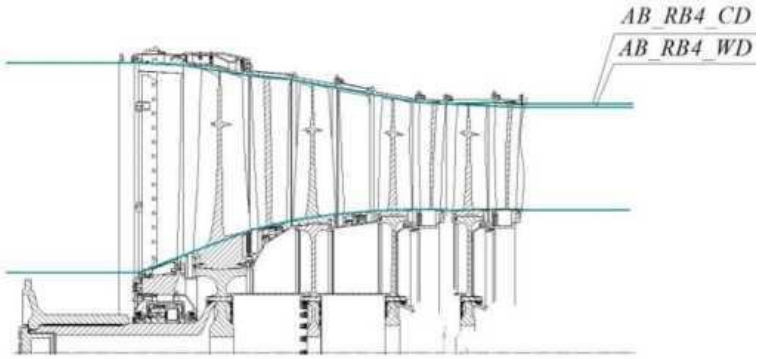

Figure 6. Four stage air brake.

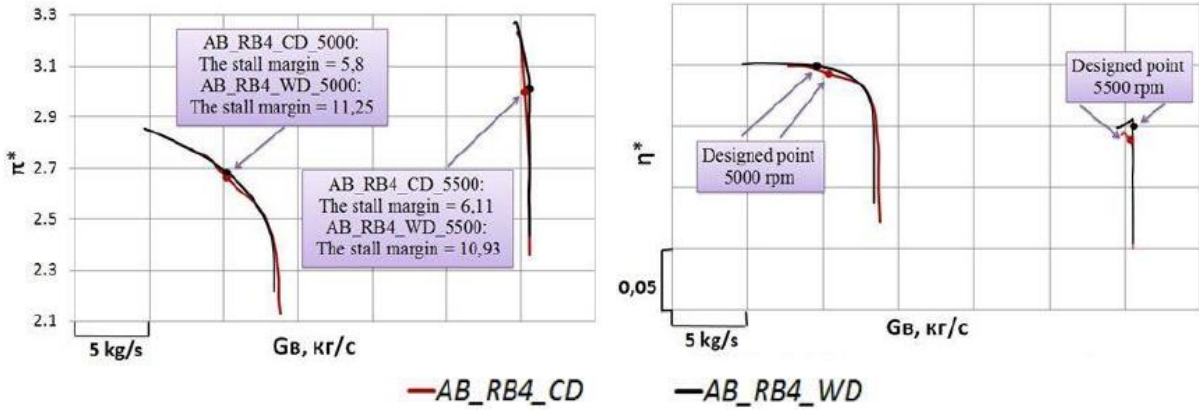

Figure 7. Head characteristics and efficiency of the air.

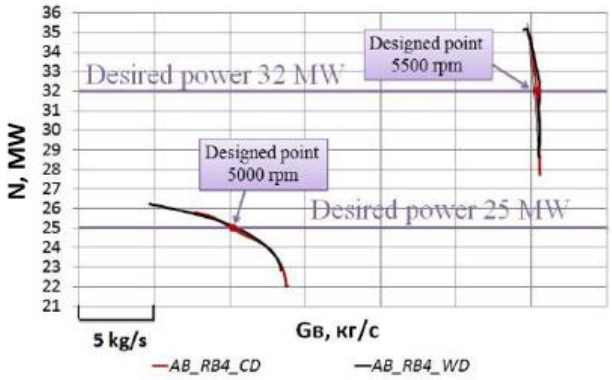

Figure 8. Characteristics of the four stage air brake.

Figure 7 shows that the air brake variant designed by duplication of the last stage, allows to utilize the required power, but it has a low stall margin. At the operation mode of 5000 rev/min the factor of the stall margin is 5,8 %, at the operation mode of 5500 rev/min factor of the stall margin is 6,11 %.

Analysis of flow structure shows that there is flow separation the hub of fourth rotor blade (Figure 9). This flow separation also expands also to the fourth GV, apparently, it is the reason of the stall margin limitation.

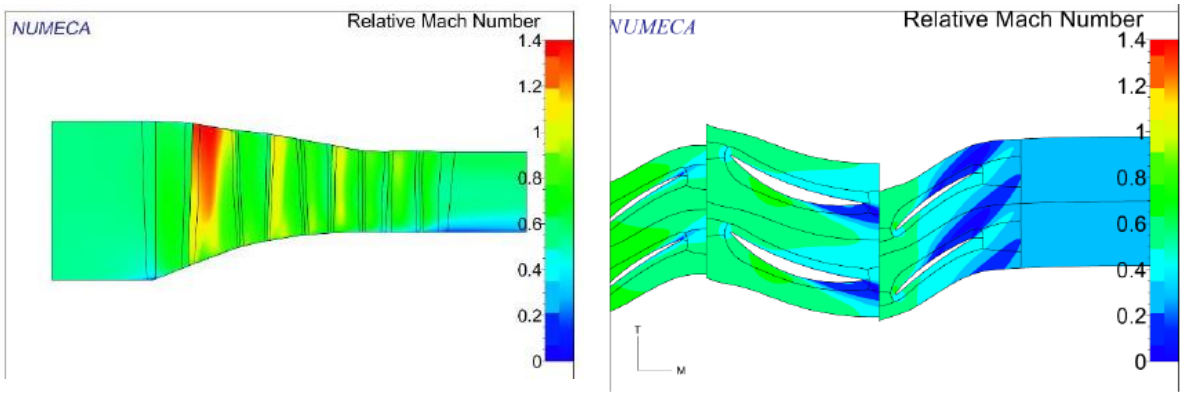

Figure 9. The flow picture of the flow in the hub section of the air brake fourth stage (at operation mode of 5500 rev / min at the operating point).

It was decided to bring waisting of the shroud of the flow channel of the fourth stage. Waisting was carried out by changing shroud of a flow channel of the fourth stage. Hub contours was remained unchanged. Designed air brake arrangement with waisting of the flow channel is shown in Figure 6 (AB_RB4_WD).

Figure 7, 8 shows plots of the characteristics comparing of the air brake variant with waisting of the flow channel and without it.

As it can be seen from the comparison of the characteristics which is illustrated in Figure 7, the stall margin was increased to an acceptable level of 11,25 % at the operation mode of 5000 rev / min and up to 10,93% at the operation mode of 5500 rev / min by the waisting implementation. Improving of the air brake performance by the waisting implementation is also confirmed by the analysis of fields of calculated Mach numbers on the hub section (Figure 10). The flow separation was eliminated.

Air brake with waisting of the flow channel was selected for further investigation. This variant has one disadvantage. The existing third GV should be modified for addition of fourth GV, but it allows providing required stall margin.

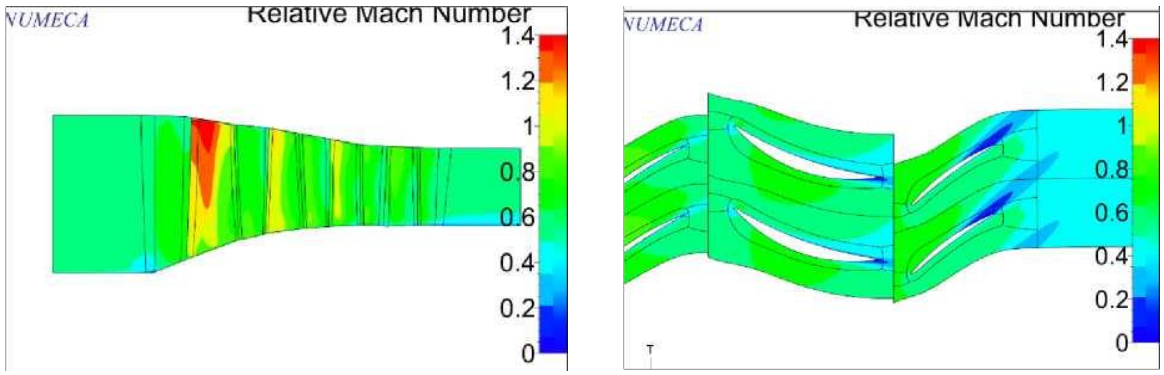

Figure 10. The flow picture of the flow in the hub section of the air brake fourth stage with waisting of the flow channel (at operation mode of 5500 rev / min at the operating point).

4. Designing of the outlet guide vane

The four-stage air brake with waisting of the flow channel allows to utilize the required power at the operation modes. However, in this configuration, there is a residual twist angle of the flow beyond the last guide vanes. The angle of the flow core in the section at fourth GV outlet at both operation modes is about 31 degrees.

Residual twist beyond the fourth GV is undesirable because it can lead to the instability work of the output devices of the air brake and test rig as a whole. It was decided to design the Outlet Guide Vane (OGV) for elimination of residual flow swirling.

To reduce OGV production costs it was decided to make it with constant cross-section height. Upon request, GV was made of 4 mm thick plate by stamping and subsequent processing of edges. In order to prevent the flow breakdown from the GV back not only in the flow core, but also in the hub and the shroud areas, it was decided to make OGV with an inlet vane angle of 36 degrees. Output vane angle was determined by the condition that the residual flow twist beyond OGV should not exceed 3 degrees. Considering the flow lagging it was decided to make the OGV output guide vanes angle equal to -2 degrees. Based on above requirements, the design of OGV was perfomed. Flow straightener cross section shown on Figure 11. The number of blades was chosen by the condition of optimum blade profiles density of mesh [7] and it was equal to 56.

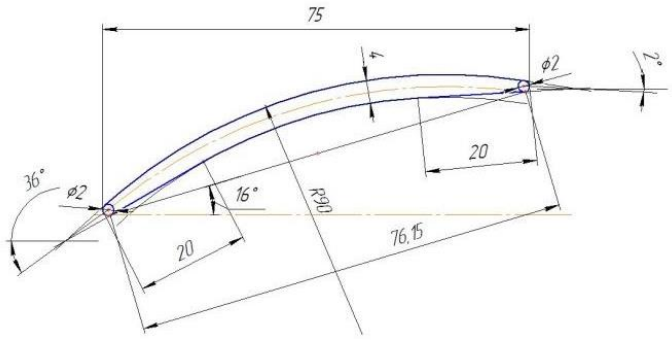

Figure 11. Geometry of the designed OGV.

The meridional profiles of the OGV were determined by design considerations. Thus, the inclination angle of the hub shroud was equal to 7 degrees to provide placing underneath it the required number of unloading disks and cavities. Unloading disks and cavities requireB to place beyond the 4th blade wheel of the air brake in order to reduce the axial force acting on the ball bearing. The angle of the shroud was chosen to be 10 degrees for the narrowing of flow channel. Created air brake configuration is shown in Figure 12.

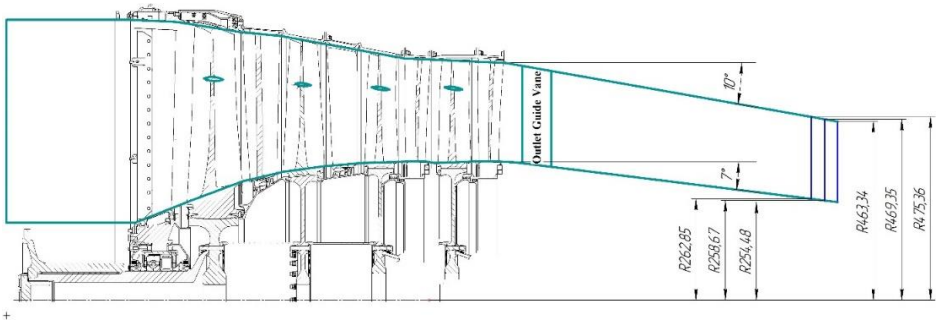

Figure 12. The air brake variant with OGV and with exhaust system.

In order to evaluate the gas-dynamic parameters of the air brake with OGV the calculation of its performance was made (Figure 13, 14). Analysis of the performance showed that this air brake configuration has stall margin 10.66 at 5000 rev / min and 9.01 at 5500 rev / min. However, the angle of the flow beyond OGV was 3 degrees.

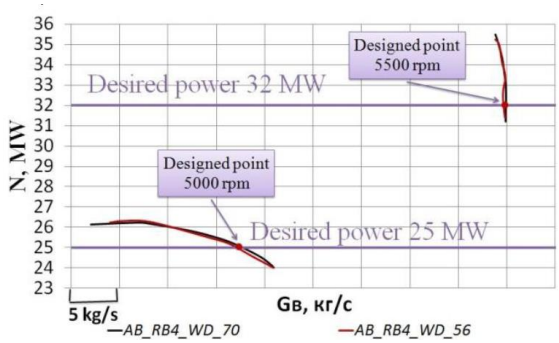

Figure 13. Characteristics of the four stage air with different numbers of OGV blades.

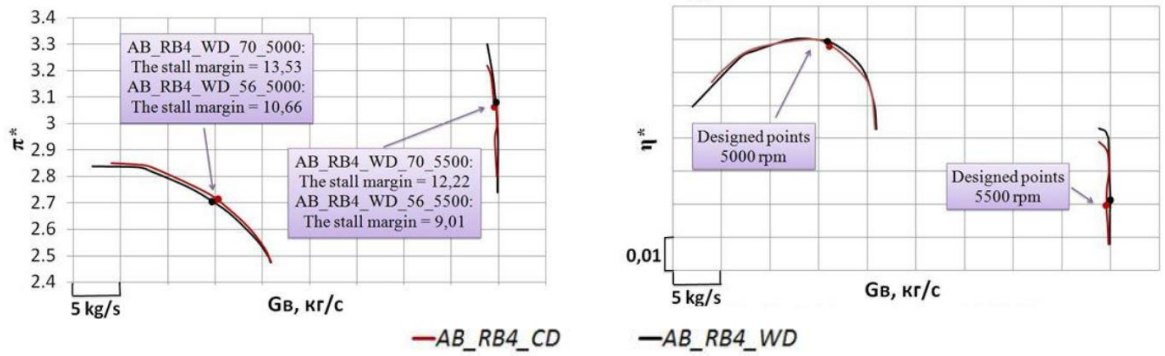

Figure 14. Head characteristics and efficiency of the air brake with different numbers of OGV blades.

Analysis of the flow structure in the air brake showed that the air brake arrangement configuration AB_RB4_WD_56 has flow separation on the hub of the OGV (Figure 12). It has been suggested that this flow separation reduces the stall margin of the air brake. It was decided to increase blade number of OGV to 70 (the air brake configuration AB_RB4_WD_70.) for reducing flow separation. Actually, this decision led to the increase in losses in the straightener (generally, profile losses), but in terms of the air brake it is not critical, because its mission is energy utilization.

Analysis of the air brake AB_RB4_WD_70 characteristics showed that the increase in number of OGV allows to increase stall margin up to 13.53% and 12.22% on operation modes 5000 rev/vin and 5500 rev/min. It also and reduce the flow separation breakdown in the OGV. Moreover, increasing the number of OGV blades has reduced cross-sectional flow angle at the output from the air brake. The output flow angle of the air brake was equal to 0 degrees.

5. Designing of the air brake exhaust system

The variable static pressure at outlet of the air brake calculation model was set during calculating of the characteristics of the air brake in parts 3 and 5 of this paper. In real operating conditions the ambient pressure will not change and will be equal to atmospheric pressure [9]. For this reason, for the air brake work it is necessary to design the special exhaust system. Mission of the exhaust system is to provide the required level of backpressure at the outlet of the air brake. The backpressure is required for the required power utilization by the air brake (the air brake operation in the required points on the characteristics).

In the case of considered configuration of the air brake the simplest exhaust device is a conical converging nozzle with a central body (Figure 12). When the nozzle works at the supercritical drop (the pressure ratio is more than 1.86) at the nozzle exit (narrowest cross section is Ni) the flow speed becomes equal to the speed of sound, and the air flow rate through the nozzle reaches a maximum possible value

and the increase of the drop at the nozzle the flow rate does not increase. Thus, the flow rate is set by the constant flow rate through the entire system as a whole: and through the nozzle and through the air brake.

For the design of the nozzle it was necessary to determine the its area of the narrowest cross section Ni by condition of the supercritical flow of air from nozzles at each of the two operation modes (N5000 of rotational speed 5000 rev / min, N5500 of rotational speed 5000 rev / min) (1). So, the total pressure, total temperature, mass flow rate was measured at the outlet from the air brake (in cross section S) at the operating points at rotational speeds of 5000 rev / min and 5500 rev / min. Measurement of flow parameters was performed using computational models described in the part 4 of this paper. The values of the measured parameters are shown in Table 1.

Table 1. The results of the parametric IPC model calculation.

n, rev/min	T_{S1}*, K	p_{S1}*, Pa	G_a, kg/sec	N, MW
5000	395.3	268597	246.85	25
5500	411.1	291132	274.97	32

The area of the narrow section at each operation mode was determined by the formula:

$$F_C = G_{S1} \cdot T_C^{*\frac{1}{2}} \cdot \left(m_g \cdot p_C^* \cdot q(\lambda_C) \cdot \mu_C\right)^{-1}. \quad (1)$$

Outer and inner diameters of the nozzle with a central body considering the meridional profiles designed in the previous step were determined after determining the areas. The calculated areas of the nozzles for each operation mode and outer and inner diameters are given in Table 2. The figure 12 shows the arrangement of the calculated nozzles together with the air brake.

Table 2. Throat areas and diameters of the air brake nozzle

n, rev/min	F_C, m^2	D_h, m	D_w, m
5000	0.471	0.509	0.927
5500	0.493	0.526	0.951

Since the cross-sectional areas for operation modes of 5000 rev / min and 5500 rev/ min are not significantly different (less than 5%), it was decided to design a one, unified nozzle (Figure 12). Use of the one unified nozzle though move working points of the air brake further from originally design points on performance map, but it can reduce the manufacturing cost (it is necessary to produce not two nozzles, but one), and it simplifies the process of the engine tests with the various powers (not need to change the exhaust nozzle during the engine replacement or the switching the operation mode at the testing engine) [10].

The combined CFD - model of the air brake with a nozzle (Figure 15) was created to check the correctness of the decision about the using of the one, unified exhaust nozzle. Designed model included the air brake, the nozzle and attached volume for correct flow modeling in the nozzle. At the inlet of the calculation model (the inlet of the air brake) the total pressure of 101325 Pa and total temperature 288.15 K were set. At the outlet of the model static pressure is equal to atmospheric pressure was set. (Figure 15). Calculation was made for two operation modes of 5000 rev / min and 5500 rev / min.

As a result of the calculations the integral parameters of the air brake at the two operational modes, considering combined its work with the nozzle were determined. Obtained operating points of the air brake with the nozzle at operation modes of 5000 rev / min and 5500 rev / min were plotted to the corresponding characteristics (Figure 17). From the analysis of the figure it can be concluded that:

1) the air brake power at operation mode 5000 rev/min is slightly less than design power and is equal to 24.8 MW;

2) the air brake power at operation mode 5500 rev/min is slightly more than design power and is equal to 32.3 MW.

The resulting deviation of the working capacity from the designed is feasible and it can be taken into account during testing of engines.

The figure 16 shows the averaged the field of Mach numbers in the circumferential direction in the coupled air brake system with nozzle at the operation mode of 5500 rev / min. From the analysis of the fields of Mach numbers it can be seen that at the nozzle outlet the flow speed is equal to the speed of sound M = 1.

The unified nozzle was designed. This nozzle allows to provide air brake operation on required modes.

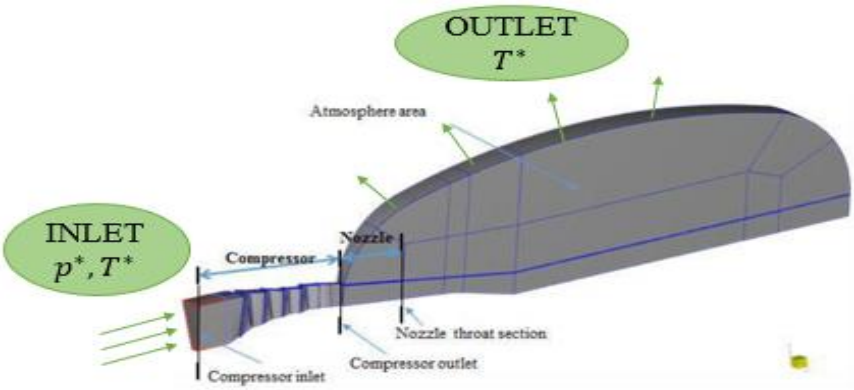

Figure 15. Calculated coupled model with the air brake exhaust device.

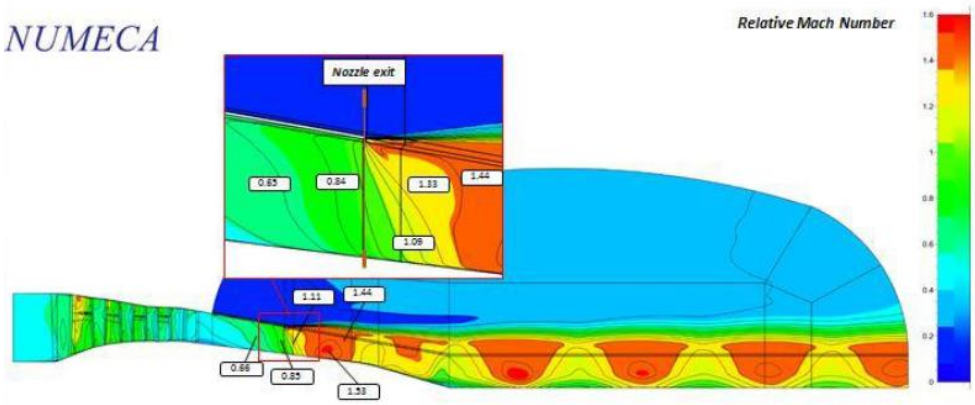

Figure 16. The field of the calculated relative Mach number of the coupled model of the air brake and exhaust nozzle.

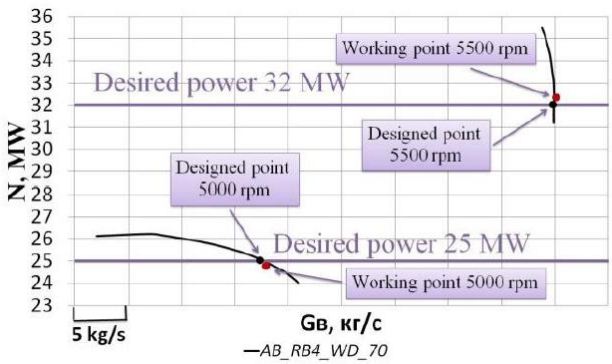

Figure 17. The air brake power characteristics with the account of the exhaust arrangement.

Conclusion

The design of the air brake was created for industrial GTE tests with the power of 25MW and 32 MW. The development of the air brake had a number of features:

1) the development was carried out using CFD - program Numeca FineTurbo. However, there was not any preliminary calculations of the turbomachinery using 1D / 2D – methods;
2) the development was carried out, mainly, using the existing parts and assemblies.

These features helped to reduce the development time, and reduce the cost of development and production of the air brake.

During the designing of the air brake the following problems have been successfully solved:

1) the workflow model of the three-stage LPC was created and its validation was made;
2) stall margin of the air brake were increased by waisting of the meridional flow channel;
3) OGV was profiled which eliminates the twist beyond the air brake;
4) unified nozzle was designed which provides the air brake work at necessary points on the characteristics.

References

[1] Korotov, M. V., "Method for testing gas-turbine engine and device for its realization", Patent of Russia Federation, RU 2318195, Date of publication 20.06.2003.
[2] Kuzmenko M.L., Egorov I.N., Shmotin Yu. N., Kretinin G.V., Fedechkin K.S., 2010, “Optimization Studies of the Aircraft High-Bypass ratio Turbo Engine Fan,”, Conference ASME Turbo Expo 2010, Glasgow, Scotland, UK, June 14-18.
[3] Kuzmichev, V S., Rybakov, V N., Tkachenko, A. Y, Krupenich, I. N., 2014, "Optimization of working process parameters of gas turbine engines line on the basis of unified engine core", ARPN Journal of Engineering and Applied Sciences, 9(10), pp. 1873-1878.
[4] NUMECA, "User Manual AutoGrid5" Release 8.4, NUMECA.inc., Belgium, January 2008.
[5] Zubanov VM., Shabliy L.S. and Krivcov A.V, 2014, “CFD-Modeling of Powerful Screw Centrifugal Kerosene Pump”. ASME Paper No. GTINDIA2014-8145
[6] Kuzmenko M.L., Egorov I.N., Shmotin Yu. N., Chupin P.V., Fedechkin K.S., 2006, “Multistage axial flow compressor optimization using 3D CFD code,”, 6th ASMO UK/ISSMO conference on Engineering Design Optimization, Oxford, UK, 3-4 July, 2006.
[7] Belousov, A. N., 2003, "Teorija i raschet aviacionnyh lopatochnyh mashin", Samara, Samarskii Dom Pechati p. 336c.
[8] Lewis, R. I., 1996, "Turbomachinery performance analysis" Publisher: Elsevier Science & Technology Books Pub, p. 329
[9] Kuz'michev, VS., Tkachenko, A.Y, Krupenich, I.N. and Rybakov, VN., 2014, “Composing a virtual model of gas turbine engine working process using the CAE system "ASTRA",” Research Journal of Applied Sciences, 9(10), pp. 635-643.
[10] Zubanov V. M., Shabliy L. S., Krivcov A. V, 2014, “Centrifugal kerosene pump CFD-modeling”. Research Journal of Applied Sciences, 9(10), pp. 629-634.